Medical Engineering and Physics 66 (2019) 12–17

Contents lists available at ScienceDirect

Medical Engineering and Physics

journal homepage: www.elsevier.com/locate/medengphy

Combining ultrasonic and computed tomography scanning to characterize mechanical properties of cancellous bone in necrotic human femoral heads

Yue Yue[a,1], Haisheng Yang[b,1], Yan Li[c], Honggang Zhong[c], Qi Tang[a], Jiantong Wang[d], Rongtian Wang[c], Haijun He[c], Weiheng Chen[c], Duanduan Chen[a,*]

[a] School of Life Science, Beijing Institute of Technology, Beijing 100081, China
[b] Department of Biomedical Engineering, College of Life Science and Bioengineering, Beijing University of Technology, China
[c] Department of Osteoarthropathy, Wangjing Hospital, Beijing, China
[d] The High School Affiliated to Renmin University of China, Beijing, China

ARTICLE INFO

Article history:
Received 27 April 2018
Revised 30 January 2019
Accepted 1 February 2019

Keywords:
Femoral head necrosis
Ultrasonic scanning
Computed tomography
Elastic modulus
Mechanical properties

ABSTRACT

Image-based finite element modelling has been commonly used to determine the biomechanical behaviours of human femora, particularly for the diagnosis of femoral head necrosis. One of the fundamental aspects of biomechanical modelling is the relationship between bone density, which is obtained from images, and elastic modulus. While there exist some empirical equations relating density with elastic modulus, the characterization of this relationship remains incomplete, especially for necrotic femoral heads. The objective of this study was to determine the relationship between density and elastic modulus by combining ultrasonic scanning and computed tomography (CT). Bone specimens were surgically removed from the femora of eight persons (seven females and one male in the age range of 55–68 years old) and underwent both ultrasonic and CT scanning. The images were processed with MATLAB scripts, and a bilinear interpolation algorithm was used to determine the relationship between the CT-measured densities and ultrasound-measured elastic moduli. The results showed different density–elastic modulus relations between the hardening strap of the necrotic region and non-hardening strap areas of the necrotic region. The uniqueness of this study is the characterization of mechanical properties (in the present study, the density–modulus relationship) from clinical images, which would be valuable in computational biomechanics used for the diagnosis and treatment evaluation of femoral head necrosis.

1. Introduction

Finite element (FE) analysis has been widely used to study the biomechanics of human femora [1–4], especially for assessing femoral implantation and treatment of osteonecrosis of the femoral head (ONFH). Typically, FE models require the assignment of bone material properties (e.g., elastic modulus) that derive from the bone mineral density, which can be determined by computed tomography (CT) scanning. One of the most important factors regarding the accuracy of an FE analysis is the utilization of a proper density–elastic modulus formula for the FE model.

The mechanical properties (e.g., elastic modulus) and their relationship with femoral bone density can be obtained through in vitro measurements from cadavers. Traditionally, for instance, compressive tests can be performed on cubic or cylindrical specimens to measure the apparent-level elastic modulus and/or bone strength, which can be related to the measured apparent densities of the specimens [5,6]. Based on those established empirical apparent-level density–modulus relationships, some studies have employed strain gauge measures and mechanical tests on whole bones (such as femora) in combination with CT scanning and FE modelling to validate and determine the most appropriate density–modulus relationships for subject-specific FE models [7–12]. In addition to mechanical testing and computational modelling, ultrasonic techniques have been used to scan cubic or cylindrical femoral samples to directly measure their elastic moduli [13–19]. Moreover, ultrasonic measures, being non-invasive, may offer some advantages over mechanical tests [20]. A few studies have combined CT and ultrasonic scanning to determine the density–modulus relationship for cortical and cancellous bone [20,21].

* Corresponding author.
E-mail address: duanduan@bit.edu.cn (D. Chen).
[1] Both authors contributed equally to this work and should be considered co-first authors.

https://doi.org/10.1016/j.medengphy.2019.02.002
1350-4533/

It should be noted that previous studies only measured the average/apparent density and ultrasound-based modulus for an entire specimen, based on which the density–modulus relations were established [21]. However, since the material property assignment in finite element modelling requires a density–modulus relationship for pixel-sized elements, those established relations might have ignored finer details of bone material properties. To the best of the authors' knowledge, no study has used a combination of ultrasound and CT to measure the material properties of necrotic bones, and no density–modulus relationships have been established for necrotic bone tissues in the literature. This is an important issue because the material property assignment is a fundamental step for finite element modelling of necrotic femora for the diagnosis of femoral head necrosis or for the prediction of femoral head collapse. Since it would be difficult to extract a small necrotic bone sample from the femur and conduct mechanical tests on it, noninvasive ultrasonic scanning of a whole femur would be a better way to measure the material properties for necrotic bone tissues.

Therefore, the current study mainly aimed to determine the relationship between density and elastic modulus for the femoral head from normal subjects and patients with femoral head necrosis by using the ultrasonic scanning technique together with CT imaging. The combination of ultrasonic and CT scanning would enable the determination of the density–elastic modulus relationship at a relatively small scale (e.g., pixel/element size), which could be more feasible for CT-based finite element modelling.

2. Materials and methods

All bone specimens were derived from eight patients, which were provided by Wangjing Hospital (seven females and one male in the age range of 55–68 years old), including seven specimens with femoral head necrosis (one male and six females) and one normal specimen (female). The sample collection procedure was approved by the Ethics Committee of the China Academy of Chinese Medical Sciences in Wangjing Hospital. The normal specimen was collected from a patient who underwent femoral head replacement due to accidental trauma instead of femoral head necrosis. The patients had received similar surgeries for femoral head replacement. The femoral specimens were selected from the upper end of the femoral neck. In other words, the entire femoral head was used as a specimen in this study. In addition, the femoral head specimens had bone marrow containing a large amount of fat, which could affect the ultrasonic imaging and thus affect the accuracy of the material property determination. For this reason, the specimens were defatted and embedded. Defatting has been reported to have a small effect on ultrasonic measurements [19]. The overall experimental process is shown in Fig. 1. In the experiment, all specimens were embedded in PMMA, which could protect the specimen skeleton and prevent infectious disease transmission. In fact, only the outside of the specimen was covered with PMMA; the PMMA did not emerge into the inner tissues of the specimen.

The femoral head portion of each tissue sample was scanned with a CT scanner (GE Medical Group, Netherlands; 120 kV, 300 mA, 1.25 mm section thickness, 0.625 mm scanning spacing and 0.5×0.5 mm pixel pitch). All CT data from the eight femoral head specimens used in the experiment were derived from the last CT scans prior to femoral head removal surgery, such as hip replacement (Fig. 2(a)). The density information of the femoral heads [8] were obtained from CT images based on the Hounsfield unit (HU) scale.

All the embedded specimens were sliced into seven pieces prior to ultrasonic scanning to ensure that there was one piece containing the largest necrotic area, and the number of pieces on both sides of this position is the same. Sectioning was performed because the ultrasonic scanning was performed perpendicular to the surface of the slice. Additionally, imaging should ensure that the specimen thickness of the scanned surface is uniform. The slicing sections corresponded to CT scans of the same patient. Before slicing, each femoral specimen was placed with the same orientation of the femoral head during the CT scanning by a professional surgeon who performed the femoral head surgery. The specimen was then fixed onto a corresponding rectangular glass sheet. The surgeon chose the relevant positions for the femoral head specimen based on prior CT scans with the greatest femoral head area on the coronal section of the necrotic femoral head and normal femoral head. Each femoral head section was 0.625 mm in thickness. The CT scanning film with the greatest femoral head area was selected from the CT films of each patient, and three CT scanning images were selected from both the anterior and posterior parts of this CT film on the coronal plane. Among them, these six CT scanning images were drawn from every other two CT scanning images, which were selected as the femoral head specimen sections for ultrasonic imaging. It was noteworthy that each section contained both the necrotic part and intact parts during the selection of femoral head specimen sections.

Ultrasonic scanning was conducted on the prepared femoral head specimens. The specimens with femoral head necrosis are the femoral heads that may include both necrotic bone and normal bone tissues, which were identified by a professional surgeon according to the diagnostic method proposed by the Japan Ministry of Health and Welfare Osteopathic Research (JIC) and Mont. The instrument was a custom-made MUT-2 scanning ultrasonic microscope [22] developed by Tsinghua University, which has a spatial resolution of 10 μm and a highest probe frequency of 130 MHz. Each scanning point was tested according to the following procedure: (1) a 130 MHz acoustic impulse was produced; (2) the ultrasonic echo was delayed before it was received; (3) the received voltage waveform corresponded to the acoustic impedance. All scanning points were automatically tested using the computer-controlled three-dimensional step scanning platform.

Following ultrasonic and CT scanning, custom-made MATLAB scripts were developed to process the CT and ultrasonic images to relate the densities with elastic moduli. The density was calculated from HU values in the CT scans based on Eq. (2.1), where ρ was the apparent density (g/cm^3), and A and B are coefficients that could be calculated by the least squares method.

$$\rho = A + B * HU \tag{2.1}$$

The elastic modulus (E) of the scanning test point was obtained from the ultrasonic scans, based on Eq. (2.2), where Z is the acoustic impedance of each scanning point of the bone samples formula after calibration with the standard material (in the present research, water at room temperature), and c was the endosseous speed of sound.

$$E = Z * c \tag{2.2}$$

Specifically, the image coordinate positions were registered between the ultrasonic and CT images to determine the density and its corresponding elastic modulus for each pixel. In the experiment, ultrasonic scanning (Fig. 2(b)) was applied to determine the elastic modulus of the cancellous bone of the femoral head. Image data were processed. To reduce the magnitude of difference between the density and elastic modulus, this study attempted to carry out matrix partitioning of the two-dimensional array information from the ultrasonic scan pictures with various matrix sizes, such as 10×10, 20×20 and 20×40. In addition, the image was scaled by using MATLAB, and the processing of each ultrasonic scan image was simplified using the bilinear interpolation algorithm. Moreover, the resolution of the ultrasound scan image was reduced to

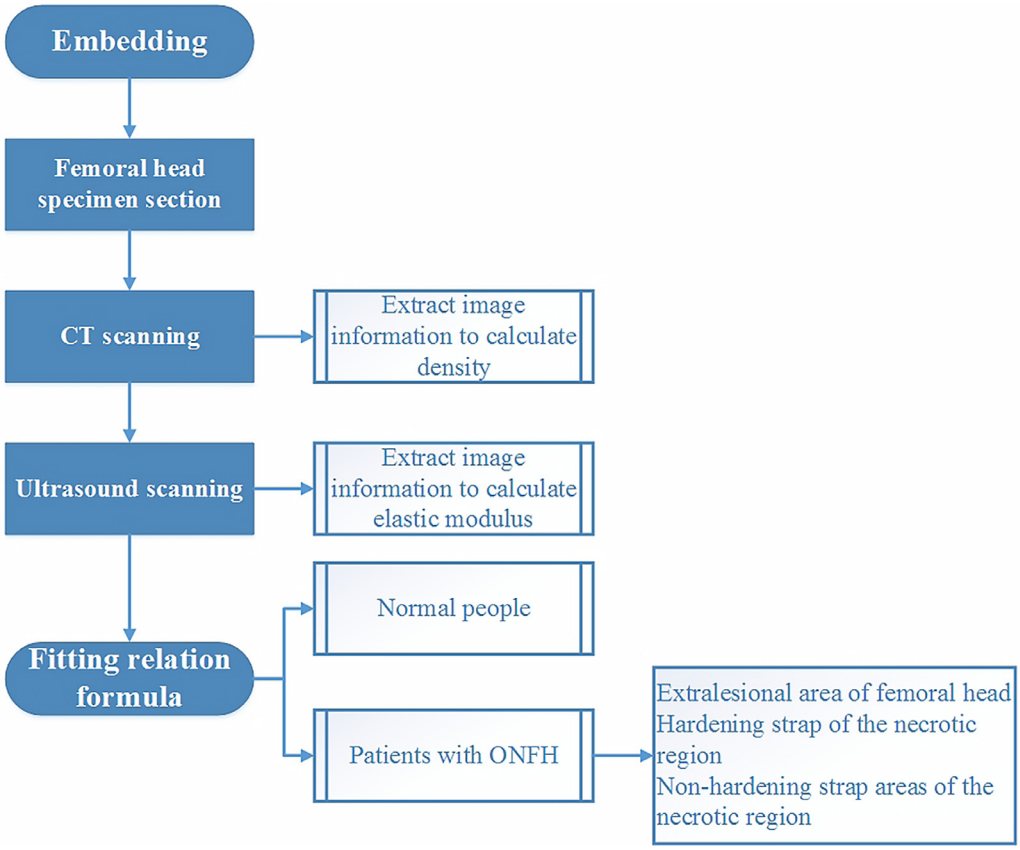

Fig. 1. Procedure of characterizing the mechanical properties (in the present study, the density–elastic modulus relationship) of cancellous bone in the human femoral head by combining CT and ultrasonic scanning.

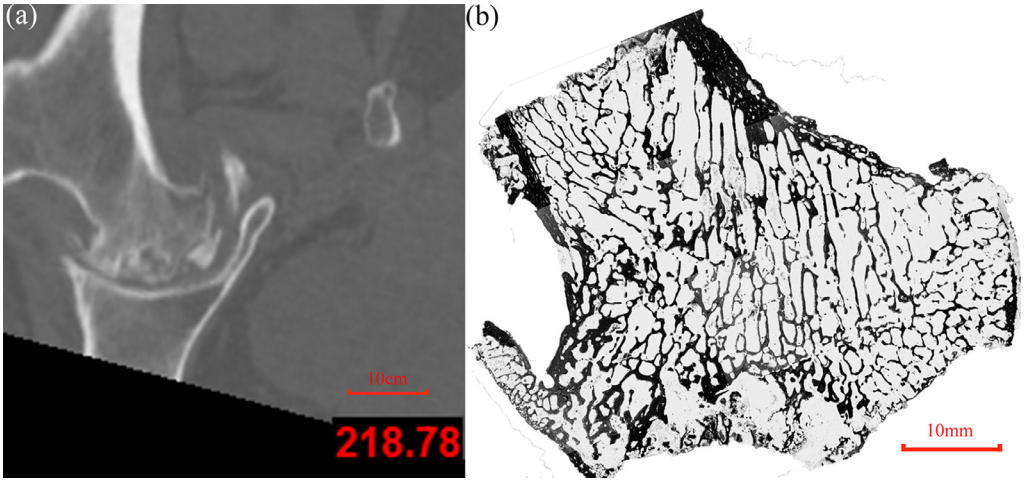

Fig. 2. (a) A computed tomography scan of a femoral sample. (b) An ultrasonic scan of the femoral head of the same sample.

that of the CT scan image. After repeated tests, it was found that the sizes of matrices that could reflect the relations between the density and elastic modulus in different samples of femoral heads were different. As a result, the testers decided to use different sizes of matrices for different sample models.

In this experiment, the correlation curve of elastic modulus versus density was fitted using the least squares method. The results suggested that the formulas regarding density and elastic modulus E followed a power relationship, as shown in Eq. (2.3), where E is the elastic modulus (MPa), ρ is the apparent density (g/cm^3), and a and b can be calculated using the least squares method. Regression analyses aimed to search for the best fit of data by minimizing the square of error in every single formula [23]. Importantly, the method of least squares and the method of calculating the error sum of squares between the calculated data and actual data allowed us to easily obtain the unknown data. Moreover, the least squares method could also be applied to curve fitting.

$$E = a * \rho^b \tag{2.3}$$

With regard to the comparison of formulas for the experimental results, there were three distinct layers on the coronal section of the necrotic femoral head when studying the relationships between density and elastic modulus of patients with ONFH, namely, the extralesional area of the femoral head, the hardening strap

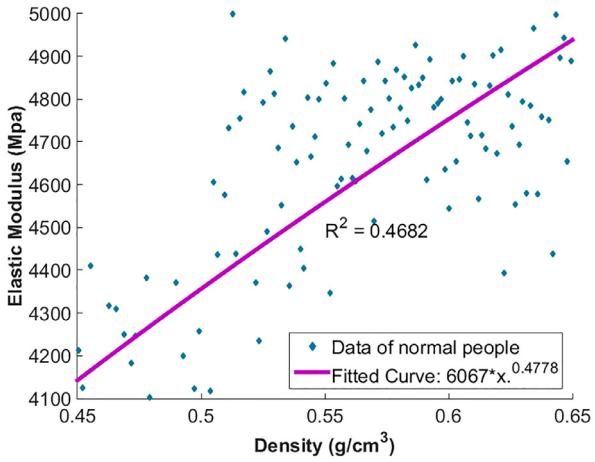

Fig. 3. Relationship between the density and elastic modulus of normal femoral heads.

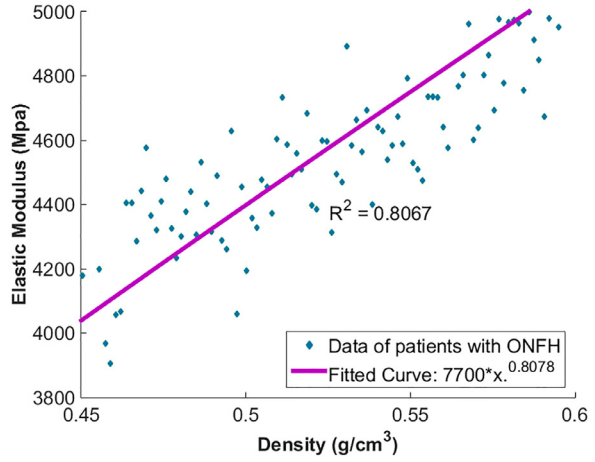

Fig. 4. Relationship between the density and elastic modulus of necrotic femoral heads.

of the necrotic region, and the non-hardening strap areas of the necrotic region. The extralesional area of the femoral head refers to the non-necrotic region in the patients with ONFH. The hardening strap of the necrotic region is shown as an area with high signal density on the CT image in the necrotic region of the femoral head in patients with ONFH. The non-hardening strap areas of the necrotic region refer to regions of necrotic lesions from gross specimens other than the sclerotic zone in patients with ONFH.

3. Results

Figs. 3 and 4 show the relationships of lattice information between the density and corresponding elastic modulus of each pixel for both normal and necrotic femoral heads. The relationships between the density and elastic modulus of cancellous bone of the normal and necrotic femoral heads corresponded to different fitted curve equations. In addition, the distribution of mechanical properties (in the present study, the density–elastic modulus relationship) was different for various samples. In the experiment, eight specimens were used, including seven specimens with femoral head necrosis and one normal specimen. There were great differences in the density–elastic modulus relationship in the extralesional areas of the femoral head between patients with and without ONFH and between the necrotic areas and sclerosis-rim areas of necrotic lesions from the gross specimens. Thus, the following conditions were considered.

First, a comparison of density–elastic modulus relations between the extralesional areas of necrotic femoral heads and normal femoral heads was performed. In the data analysis, relation diagrams were drawn on the basis of the mean elastic modulus and density. Parameters $a = 6710$ and $b = 0.5369$ for one curve representing extralesional areas of necrotic femoral heads, which were greater than those for another curve on normal femoral heads wherein $a = 6067$ and $b = 0.4778$; this result indicates that gradual calcification of normal cancellous bone in the femoral heads of the patient might occur even if the CT data from a patient with ONFH did not reveal necrotic lesions (Fig. 5(a)).

Second, according to a comparison of the density–elastic modulus relations between the hardening straps and non-hardening strap areas of the necrotic region, in both $a = 14{,}540$ and $b = 0.6214$ for one curve and $a = 5415$ and $b = 0.1928$ for another curve, which indicates differences between the sclerosis-rim areas and non-hardening strap areas (Fig. 5(b)). Therefore, the material properties of sclerosis-rim areas were different from those of non-hardening strap areas of necrotic lesions from gross specimens. Moreover, the curves for the sclerosis-rim areas were significantly higher than those of the entire necrotic areas and non-hardening strap areas of the necrotic region. This result indicated that hardening straps of a femoral head had the highest elastic moduli in the femoral heads of patients with femoral head necrosis.

Additionally, comparisons of density–elastic modulus relations of all areas of normal and necrotic femoral heads were conducted. When the densities were low, the parameters $a = 7700$ and $b = 0.8078$ for one curve corresponding to a patient with ONFH, which were lower than those for another curves corresponding to a normal subject wherein $a = 6067$ and $b = 0.4778$ (Fig. 5(a)). However, when the densities increased to $0.49\,g/cm^3$, the curves from the normal patients were significantly lower than those of the patients with ONFH.

Lastly, when the densities were low, the curves of the non-hardening strap areas of the necrotic region were higher than those of their extralesional areas (Fig. 5(b)). However, when the densities increased to $0.53\,g/cm^3$, parameters $a = 5415$ and $b = 0.1928$ for one curve for non-hardening strap areas were significantly lower than those for the curve for their extralesional areas wherein $a = 6710$ and $b = 0.5369$.

4. Discussion

The present study investigated the relationship between density and elastic modulus by combining ultrasonic and CT scanning. The formula between density and elastic modulus determined in this study is of great importance in computational modelling to study the biomechanical behaviours of femoral heads. These experimental results indicated that, for patients with osteonecrosis of the femoral head, the relationships between density and elastic modulus were different among three typical regions, namely, the extralesional area of the femoral head, the hardening strap of the necrotic region, and the non-hardening strap areas of the necrotic region. Additionally, the relationships between densities and elastic moduli were different in the normal regions between subjects with normal femoral heads and patients with ONFH.

In the experiments, the entire femoral head was sliced. The elastic moduli of the bone tissues in the femoral head were obtained based on each pixel at a microscale. The density and elastic modulus were extracted based on each pixel mainly because the femoral bone tissue was an anisotropic material, which could be regarded as an isotropic material in this study when being considered at a dimension of a few hundred microns. Compared with research based on a small cube in the femoral head that determined density through simple weighing and volumetric measurement, this experimental method could more precisely determine

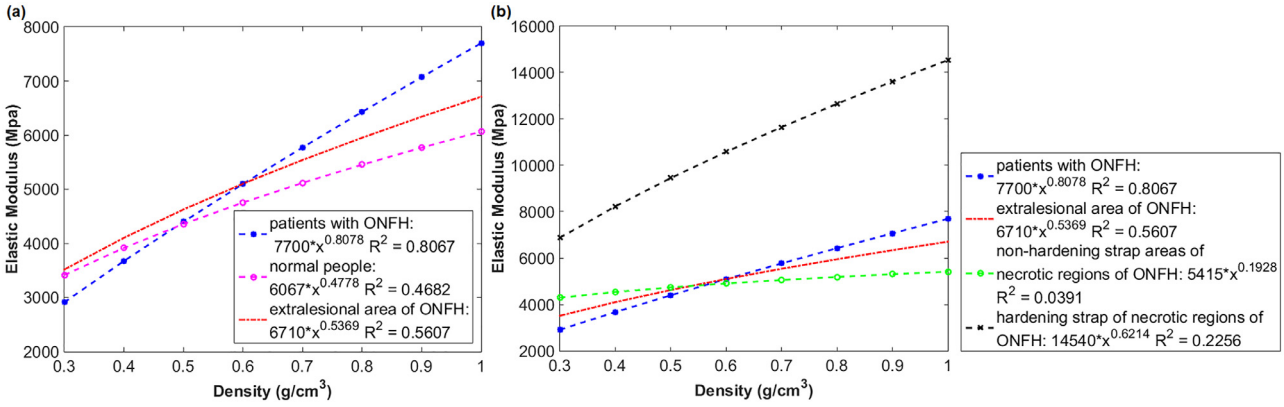

Fig. 5. (a) Relationship between the density and elastic modulus of normal regions of all specimens, including normal and necrotic femoral heads. (b) Relationship between the density and elastic modulus of the necrotic femoral head specimens, including 6 from female patients and 1 from a male patient.

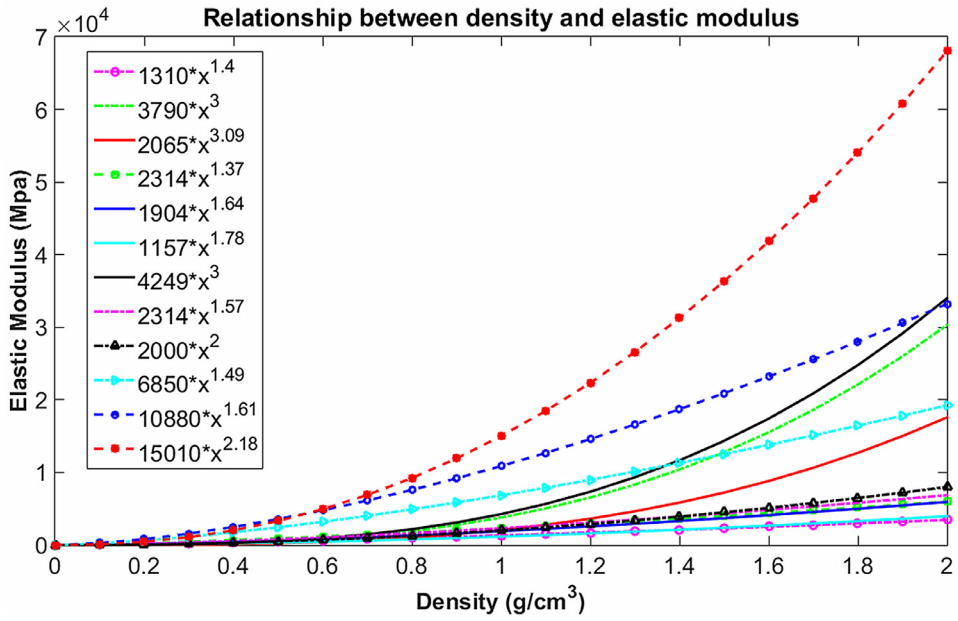

Fig. 6. Correlation curves and formulas between the density and elastic modulus determined in previous studies [5,20,24–30].

the density and elastic modulus at a relatively smaller scale, which enables fitting the formula regarding the relationship of the density with the elastic modulus.

It was found in this experiment that the regions of necrotic lesions from gross specimens in patients can be divided into two regions for discussion: the hardening strap in the necrotic region and the non-hardening strap areas of the necrotic region. As can be discovered from this experiment, the relationship between the density and elastic modulus in the hardening strap of the necrotic region was obviously different from that in non-hardening strap areas of the necrotic region. Therefore, it is suggested to define these two regions separately for the sake of accuracy in subsequent femoral head biomechanical modelling. For the moment, the authors attempted to compare the relationships between the densities and elastic moduli described in previous studies [5,20,24–30] with those in this research (Fig. 6). The results demonstrated that the exponent in the exponential function relationship existing between femoral head density and elastic modulus obtained in this experiment was less than 1, whereas this exponent was greater than 1 in previous studies [5,20,24–30]. In addition, one potential limitation of this study was that the limited sample size in the experiment might affect the accuracy of calculating the coefficients a and b in the relationship formula between density and elastic modulus.

Limitations of this study include a relatively small sample size, skewed gender ratio (7 females and 1 male) and only one normal sample. The main reason behind this was that it was difficult to collect both necrotic and normal femoral head samples that satisfy the requirements of the proposed experiments. Although femoral head necrosis is a common disease and many patients undergo total hip replacements, most replaced femoral heads with necrosis are severely collapsed and thus they are not suitable for further experiments or measurements. However, collecting normal samples is even more challenging. Most of the normal femoral head subjects of humans were from femoral neck fractures. However, only a few patients with femoral neck fractures underwent hip replacement surgery. Moreover, some patients with femoral neck fractures also suffer from other types of diseases of the femoral head, which makes it more difficult for human normal femoral heads to be recruited. In the current study, each human femoral head subject was cut into seven slices. Nevertheless, testing the cut samples from a limited number of specimens was commonly applied in previous studies [21,31–34]. A future study with a greater sample size would be warranted to address this issue.

5. Conclusions

In summary, this paper has determined the density–modulus relationships of femoral cancellous bone from eight human subjects using an ultrasonic scanning technique. The density–elastic modulus relationships for femoral bone tissues of normal patients and patients with osteonecrosis of the femoral head were determined. In addition, experiments have been carried out to categorize the necrotic and normal regions from patients with ONFH to obtain their respective relationship formulas between density and elastic modulus. The density in the formula is obtained through CT scanning, whereas the elastic modulus is acquired via ultrasonic scanning. The results showed different biomechanical properties and density–elastic modulus relations among the extralesional area of the femoral head, hardening strap of the necrotic region, and non-hardening strap areas of the necrotic region.

Acknowledgments

This study was supported by National Key R&D Program of China (2017YFC0107901), National Natural Science Foundation of China (81770465, 11702008), Support Plan for High-level Faculties in Beijing Municipal Universities (CIT&TCD201804011) and Beijing Excellent Talents Funds (2017000020124G277).

Conflict of interest

There is no conflict of interests in this study.

Ethical approval

WJEC-KT-2016-007-P002
China Academy of Chinese Medical Sciences Wangjing Hospital.

References

[1] Baca V, Horak Z, Mikulenka P, Dzupa V. Comparison of an inhomogeneous orthotropic and isotropic material models used for FE analyses. Med Eng Phys 2008;30(7):924–30.
[2] Keyak JH, Meagher JM, Skinner HB, Mote CJ. Automated three-dimensional finite element modelling of bone: a new method. J Biomed Eng 1990;12(5):389–97.
[3] Keyak JH, Skinner HB. Three-dimensional finite element modelling of bone: effects of element size. J Biomed Eng 1992;14(6):483–9.
[4] Yang H, Ma X, Guo T. Some factors that affect the comparison between isotropic and orthotropic inhomogeneous finite element material models of femur. Med Eng Phys 2010;32(6):553–60.
[5] Carter DR, Hayes WC. The compressive behavior of bone as a two-phase porous structure. J Bone Joint Surg Am 1977;59(7):954–62.
[6] Morgan EF, Bayraktar HH, Keaveny TM. Trabecular bone modulus–density relationships depend on anatomic site. J Biomech 2003;36(7):897–904.
[7] Austman RL, Milner JS, Holdsworth DW, Dunning CE. The effect of the density–modulus relationship selected to apply material properties in a finite element model of long bone. J Biomech 2008;41(15):3171–6.
[8] Peng L, Bai J, Zeng X, Zhou Y. Comparison of isotropic and orthotropic material property assignments on femoral finite element models under two loading conditions. Med Eng Phys 2006;28(3):227–33.
[9] Eberle S, Göttlinger M, Augat P. An investigation to determine if a single validated density–elasticity relationship can be used for subject specific finite element analyses of human long bones. Med Eng Phys 2013;35(7):875–83.
[10] Eberle S, Göttlinger M, Augat P. Individual density-elasticity relationships improve accuracy of subject-specific finite element models of human femurs. J Biomech 2013;46(13):2152–7.
[11] Helgason B, Perilli E, Schileo E, Taddei F, Brynjolfsson S, Viceconti M. Mathematical relationships between bone density and mechanical properties: a literature review. Clin Biomech 2008;23(2):135–46.
[12] Taddei F, Schileo E, Helgason B, Cristofolini L, Viceconti M. The material mapping strategy influences the accuracy of CT-based finite element models of bones: an evaluation against experimental measurements. Med Eng Phys 2007;29(9):973–9.
[13] Ashman RB, Rho JY, Turner CH. Anatomical variation of orthotropic elastic moduli of the proximal human tibia. J Biomech 1989;22(8–9):895–900.
[14] Bernard S, Schneider J, Varga P, Laugier P, Raum K, Grimal Q. Elasticity-density and viscoelasticity-density relationships at the tibia mid-diaphysis assessed from resonant ultrasound spectroscopy measurements. Biomech Model Mechanobiol 2016;15(1):97–109.
[15] Berteau JP, Baron C, Pithioux M, Launay F, Chabrand P, Lasaygues P. In vitro ultrasonic and mechanic characterization of the modulus of elasticity of children cortical bone. Ultrasonics 2014;54(5):1270–6.
[16] Daoui H, Cai X, Boubenider F, Laugier P, Grimal Q. Assessment of trabecular bone tissue elasticity with resonant ultrasound spectroscopy. J Mech Behav Biomed Mater 2017;74:106–10.
[17] Daugschies M, Rohde K, Gluer CC, Barkmann R. The preliminary evaluation of a 1 MHz ultrasound probe for measuring the elastic anisotropy of human cortical bone. Ultrasonics 2014;54(1):4–10.
[18] Rho JY, Ashman RB, Turner CH. Young's modulus of trabecular and cortical bone material: ultrasonic and microtensile measurements. J Biomech 1993;26(2):111–19.
[19] Wear KA, Nagaraja S, Dreher ML, Sadoughi S, Zhu S, Keaveny TM. Relationships among ultrasonic and mechanical properties of cancellous bone in human calcaneus in vitro. Bone 2017;103:93–101.
[20] Rho JY, Hobatho MC, Ashman RB. Relations of mechanical properties to density and CT numbers in human bone. Med Eng Phys 1995;17(5):347–55.
[21] Grant CA, Wilson LJ, Langton C, Epari D. Comparison of mechanical and ultrasound elastic modulus of ovine tibial cortical bone. Med Eng Phys 2014;36(7):869–74.
[22] Ashman RB, Cowin SC, van Buskirk WC, Rice JC. A continuous wave technique for the measurement of the elastic properties of cortical bone. J Biomech 1984;17(5):349–61.
[23] Charnes A, Frome EL, Yu PL. The equivalence of generalized least squares and maximum likelihood estimates in the exponential family. J Am Stat Assoc 1976;71(353):169–71.
[24] Ciarelli TE, Fyhrie DP, Schaffler MB, Goldstein SA. Variations in three-dimensional cancellous bone architecture of the proximal femur in female hip fractures and in controls. J Bone Miner Res 2000;15(1):32–40.
[25] Dalstra M, Huiskes R, Odgaard A, van Erning L. Mechanical and textural properties of pelvic trabecular bone. J Biomech 1993;26(4–5):523–35.
[26] Kaneko TS, Bell JS, Pejcic MR, Tehranzadeh J, Keyak JH. Mechanical properties, density and quantitative CT scan data of trabecular bone with and without metastases. J Biomech 2004;37(4):523–30.
[27] Keller TS. Predicting the compressive mechanical behavior of bone. J Biomech 1994;27(9):1159–68.
[28] Ohman C, Baleani M, Perilli E, Dall'Ara E, Tassani S, Baruffaldi F, Viceconti M. Mechanical testing of cancellous bone from the femoral head: experimental errors due to off-axis measurements. J Biomech 2007;40(11):2426–33.
[29] Ouyang J, Yang GT, Wu WZ, Zhu QA, Zhong SZ. Biomechanical characteristics of human trabecular bone. Clin Biomech 1997;12(7–8):522–4.
[30] Taylor WR, Roland E, Ploeg H, Hertig D, Klabunde R, Warner MD, Clift SE. Determination of orthotropic bone elastic constants using FEA and modal analysis. J Biomech 2002;35(6):767–73.
[31] Grimal Q, Haupert S, Mitton D, Vastel L, Laugier P. Assessment of cortical bone elasticity and strength: mechanical testing and ultrasound provide complementary data. Med Eng Phys 2009;31(9):1140–7.
[32] Teo JCM, Si-Hoe KM, Keh JEL, Teoh SH. Correlation of cancellous bone microarchitectural parameters from microCT to CT number and bone mechanical properties. Mat Sci Eng C-Mater 2007;27(2):333–9.
[33] Ohman C, Dall'Ara E, Baleani M, Van Sint JS, Viceconti M. The effects of embalming using a 4% formalin solution on the compressive mechanical properties of human cortical bone. Clin Biomech 2008;23(10):1294–8.
[34] Katsamenis OL, Jenkins T, Thurner PJ. Toughness and damage susceptibility in human cortical bone is proportional to mechanical inhomogeneity at the osteonal-level. Bone 2015;76:158–68.